Published in IET Generation, Transmission & Distribution
Received on 16th May 2011
doi: 10.1049/iet-gtd.2011.0657

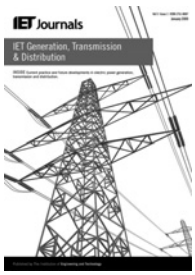

ISSN 1751-8687

Accurate fault location algorithm for transmission lines in the presence of shunt-connected flexible AC transmission system devices

M. Ghazizadeh-Ahsaee J. Sadeh

Electrical Engineering Department, Faculty of Engineering, Ferdowsi University of Mashhad, Mashhad, Iran
E-mail: sadeh@um.ac.ir

Abstract: In this study a non-iterative fault location algorithm for shunt-compensated transmission lines is proposed. Since this method does not utilise the model of the shunt compensator, the errors resulted from modelling of the shunt compensators are eliminated. In addition, the new algorithm is not an iterative one and does not require proposing a selector to determine the fault section with respect to the compensator location. In this method, synchronous data from both ends of transmission line are used and distributed parameter line model in time domain is considered. This algorithm consists of three steps. In the first and second steps, it is assumed that the fault is located on the left- and right-hand side of the compensator, respectively. Two discretised equations with respect to these steps are obtained which are used to derive an optimisation problem in the third step. The location of fault and its resistance are determined by solving this problem. This method is applicable for all transmission lines compensated by any shunt device. A 300 km/345 kV transmission line compensated by STATic synchronous COMpensator (STATCOM) simulated in PSCAD/EMTDC has been used to evaluate the performance of the algorithm. The simulation results verify the high accuracy of the method.

1 Introduction

The research of fault location has notable benefits of economy and society; and several fault location algorithms have been proposed and applied to locate the point of fault on transmission lines [1–11]. Some of the proposed methods use one-terminal data [1–3] and the others utilise two-terminal data [4–11] for fault location. In the latter methods, data measurements at different buses are acquired synchronously [4–8] or asynchronously [9–11].

Flexible AC transmission systems (FACTS) offer better power flow control and enhanced dynamic stability by controlling one or more AC transmission system parameters (voltage, phase angle and impedance). Shunt compensations (static var compensation (SVC) and STATCOM) generate or absorb reactive power at their point of connection, and for them, the voltage control scheme helps to maintain voltage and synchronous stability or to avoid voltage collapse after a major disturbance [12].

When a fault occurs, the presence of a shunt compensator in the line creates new problems for fault location algorithms and since the control system of shunt compensator reacts to the fault, the voltages and currents at the fault locator point will be affected in the transient state.

Fault location algorithms for the shunt-compensated transmission lines are presented in few articles such as [13]. In order to overcome the difficulties in the modelling of the shunt FACTS devices during the faults, the compensator model is not used in [13]. Consequently, the errors resulted from the modelling of the compensator and the uncertainties of its parameters are avoided, but this method is an iterative one and the procedure is repeated until the convergence is achieved. One difficulty with such iterative calculations is choosing initial values on which the convergence of these methods depends, and choosing incorrect initial values may cause error in results or may cause divergence of these calculations. On the other hand, for the presented method in [13], two solutions are resulted, assuming that the fault is located on the left- and right-hand side of the compensator and only one of them is correct, whereas the other has to be rejected. Hence, such algorithms require a selector to select the valid result.

In the present work, a new fault location algorithm for the transmission lines compensated by the shunt FACTS devices is proposed. This technique avoids iterative calculations and it does not need to propose a selector. In addition, this algorithm is independent of the shunt FACTS device models; therefore, this method is not influenced by the uncertainty of the shunt FACTS device models and their controller parameters. In this technique, an optimisation problem is achieved, and then the exact location of fault is determined by solving this optimisation problem. A transmission line compensated by a STATCOM is used to evaluate the performance of the algorithm. The accuracy of the proposed method is very high and the error is kept below 0.0454% in all test cases without considering errors in measurements, synchronisation and line parameters.

The rest of the paper is organised as follows. Section 2 explains the principle of the new fault location algorithm

for the shunt-compensated transmission lines. In Section 3, results of evaluation of the developed fault location algorithm and sensitivity analysis of the method are presented and discussed, using the PSCAD/EMTDC simulator. The evaluation is followed by the conclusion in Section 4.

2 Principle of the new fault location algorithm

Fig. 1 depicts a transmission line compensated by a shunt FACTS device in which a three-phase fault occurs on the left-hand side of the compensator at a distance x from the sending end (point F). Systems A and B represent Thevenin's equivalent of the external networks. A and B represent the sending and receiving end buses, respectively. In the proposed algorithm, synchronous voltage and current data from both ends of the transmission line are used. The distributed parameter line model is considered to find the location of fault. Since the DB section of the line is sound, solving the partial differential equations which represent the distributed line model of the DB section; considering the voltage and current of the receiving end data (v_B, i_B) as boundary conditions, the voltage at the right-hand side of the compensator (v_D) is calculated. Since the compensator is a shunt one and does not have any series part, the voltages at the left- and right-hand side of the compensator are equal ($v_C = v_D$). For faulty section of the line (CA section), the voltage and current of bus A (v_A, i_A) and merely the voltage of bus C (v_C) are known. The data are not sufficient for the conventional two-ended fault location algorithms, since the current of the end bus of the faulty section (i_C) is not known. Thus, in this paper, a new and accurate algorithm is presented to consider just these known data to find the location of fault. It is worthy to note that the similar condition happens if the faulty section is the DB part. In this case, the voltage of bus C can be calculated, using the partial differential equations of the line model, considering sending end data (v_A, i_A) as boundary conditions. The voltages at the right- and left-hand side of the shunt compensator are equal. Therefore v_D is also known. For this fault condition, the voltage and current of the receiving end (v_B, i_B) and merely the voltage of bus D (v_D) are known and the current of bus D (i_D) is unknown. Thus, as the previous case, the conventional two-ended fault location algorithms cannot help to find the location of fault.

Based on the above explanations, in this paper, at first a novel and accurate fault location algorithm is proposed to find the exact location of fault which utilises two-end voltage and one-end current. After that, this algorithm is used to find the location of fault in the shunt-compensated transmission line, as explained in the next subsections.

The basic principle of the proposed algorithm is described via the CA part of the transmission line for a symmetrical three-phase fault in the next section. Then this algorithm is developed for transmission lines compensated by any shunt device.

2.1 Symmetrical three-phase fault

Fig. 2 shows a single-phase model of a three-phase transmission line. It is assumed that the sending end voltage and current (v_A, i_A) and the voltage of bus C (v_C) are known and available in time domain and the current of bus C (i_C) is unknown. The voltage and current at the left-hand side of the fault point (v_{FA}, i_{FA}) can be written as a function of the sending end data as follows [14]

$$\begin{aligned} v_{FA}(t) = \Bigg(& (Z_c + R'_A/4)^2[v_A(t+\tau) - (Z_c + R'_A/4)i_A(t+\tau)] \\ & + (Z_c - R'_A/4)^2[v_A(t-\tau) + (Z_c - R'_A/4)i_A(t-\tau)] \\ & - \frac{(Z_c + R'_A/4)R'_A}{4}\left[\frac{R'_A/2}{(Z_c + R'_A/4)}v_A(t) \right. \\ & \left. + 2(Z_c - R'_A/4)i_A(t)\right]\Bigg)/2Z_c^2 \end{aligned} \tag{1}$$

$$\begin{aligned} i_{FA}(t) = \Bigg(& (Z_c + R'_A/4)[v_A(t+\tau) - (Z_c + R'_A/4)i_A(t+\tau)] \\ & - (Z_c - R'_A/4)[v_A(t-\tau) + (Z_c - R'_A/4)i_A(t-\tau)] \\ & - \frac{R'_A}{4}\left[2v_A(t) - \frac{R'_A}{2}i_A(t)\right]\Bigg)/2Z_c^2 \end{aligned} \tag{2}$$

where τ is the elapsed time for the wave propagation from A to F; Z_c the characteristic impedance; and R'_A is the line resistance from A to F.

Because of the continuity of the line and consequently the continuity of the voltage along the line, the voltage at the

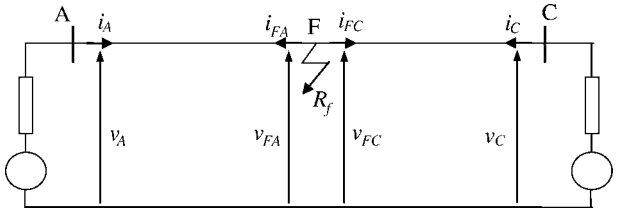

Fig. 2 *Single line diagram of a three-phase transmission line with distributed parameters*

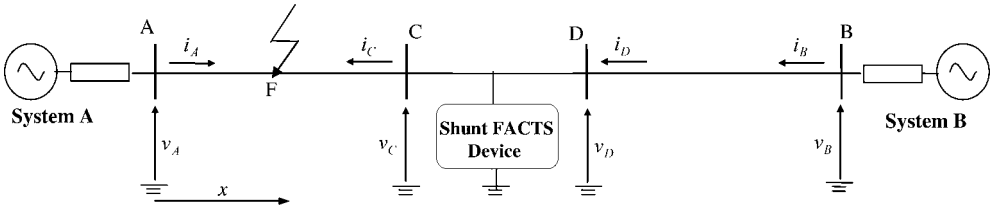

Fig. 1 *Shunt compensated transmission line; the fault occurs in the left-hand side of the compensator*

doi: 10.1049/iet-gtd.2011.0657

right-hand side of the fault (v_{FC}) is equal to the voltage at the left-hand side of it (v_{FA}). The following relation is expressed at the fault point using Kirchhoff's current law

$$i_{FC}(t) = -i_{FA}(t) - \frac{v_{FA}(t)}{R_f} \tag{3}$$

where R_f is the fault resistance.

The following equation can be obtained according to Fig. 2 [14]

$$\begin{aligned} v_C(t) = \Bigg(& (Z_c + R'_C/4)^2 [v_{FC}(t + T_A - \tau) \\ & - (Z_c + R'_C/4) i_{FC}(t + T_A - \tau)] \\ & + (Z_c - R'_C/4)^2 [v_{FC}(t - T_A + \tau) \\ & + (Z_c - R'_C/4) i_{FC}(t - T_A + \tau)] \\ & - \frac{(Z_c + R'_C/4) R'_C}{4} \Bigg[\frac{R'_C/2}{(Z_c + R'_C/4)} v_{FC}(t). \\ & + 2(Z_c - R'_C/4) i_{FC}(t) \Bigg] \Bigg) / 2Z_c^2 \end{aligned} \tag{4}$$

where R'_C is the line resistance from C to F; and T_A the elapsed time for the wave propagation from A to C.

By substituting (3) into (4), (5) is derived

$$\begin{aligned} v_C(t) = \Bigg(& (Z_c + R'_C/4)^2 \Bigg[\left(1 + \frac{(Z_c + R'_C/4)}{R_f} \right) v_{FA}(t + T_A - \tau) \\ & + (Z_c + R'_C/4) i_{FA}(t + T_A - \tau) \Bigg] \\ & + (Z_c - R'_C/4)^2 \Bigg[\left(1 - \frac{(Z_c - R'_C/4)}{R_f} \right) v_{FA}(t - T_A + \tau) \\ & - (Z_c - R'_C/4) i_{FA}(t - T_A + \tau) \Bigg] \\ & - \frac{(Z_c + R'_C/4) R'_C}{4} \Bigg[\left(\frac{R'_C/2}{(Z_c + R'_C/4)} \right. \\ & \left. - \frac{2(Z_c + R'_C/4)}{R_f} \right) v_{FA}(t) \\ & - 2(Z_c - R'_C/4) i_{FA}(t) \Bigg] \Bigg) / 2Z_c^2 \end{aligned} \tag{5}$$

Also, by substituting (1) and (2) into (5), the voltage of bus C (v_C) is obtained as a function of the voltage and current of the sending end (v_A, i_A), the elapsed time for the wave propagation from A to F (τ) and the fault resistance (R_f)

$$v_C(t) = g_1(v_A, i_A, \tau, R_f, t) \tag{6}$$

As mentioned previously, it is assumed that $v_A(t)$, $i_A(t)$ and $v_C(t)$ are known and available. So, the following equation is defined using (6)

$$G_1(v_A, i_A, v_C, \tau, R_f, t) = 0 \tag{7}$$

In this equation, there are two unknown quantities: the surge travelling time from A to F (τ) and the fault resistance (R_f). τ is proportional to the fault distance from the sending end (x)

$$\tau = \frac{x}{c} \tag{8}$$

where c is the velocity of the wave propagation.

To obtain x and R_f, at first, (8) is substituted into non-linear equation (7) and then it is discretised as follows

$$G_1(v_A, i_A, v_C, x, R_f, k) = 0 \tag{9}$$

where $k\Delta t = t$; Δt is the sampling step; and k is the arbitrary integer.

All samples in the data window should satisfy (9), at the fault point. So, by solving (9), the fault location and the fault resistance (R_f) are calculated, using two-end voltage and one-end current data.

In this subsection, the proposed method was described via the CA part of the line using the known data, which is subsequently utilised to develop the fault location algorithm for the shunt-compensated transmission lines.

2.2 Case of shunt-compensated transmission lines

Since the location of fault with respect to the compensator is unknown prior to fault location determination, the proposed method includes three steps. In the first and second steps, it is assumed that the fault is located on the left- and right-hand side of the shunt compensator, respectively. Two discretised equations with respect to the first two steps are obtained, which are finally used to derive an optimisation problem in step three. The proposed method is explained in the rest of this subsection:

Step one: Consider a shunt-compensated three-phase transmission line (Fig. 1) in which a symmetrical three-phase fault occurs on the left-hand side of the compensator. The voltage at the right-hand side of the shunt FACTS device (v_D) can be obtained using the receiving end voltage and current (v_B, i_B)

$$v_D(t) = g_2(v_B, i_B, t) \tag{10}$$

Because of non-existence of the series branch for the shunt compensator, and continuity of the voltage along the line, v_D is equal to the voltage at the left-hand side of the shunt FACTS device (v_C). So, v_C is known and the discretised equation (9) can be utilised. After discretising (10) and by substituting the result into (9), the following equation is written

$$\begin{cases} G_1(v_A, i_A, v_B, i_B, x, R_f, k) = 0 \\ 0 < x < x_{\text{Comp}} \end{cases} \tag{11}$$

where x_{Comp} is the distance of the compensator from bus A.

Equation (11) is obtained based on the assumption that the fault point is situated in the first part of the line (CA section). Therefore x is placed between the sending end and x_{Comp}.

Step two: In this step, it is assumed that the fault is located on the right-hand side of the shunt compensator (DB part). The voltage at the left-hand side of the shunt FACTS device (v_C) can be obtained using the sending end-recorded data of the voltage and current (v_A, i_A). So, the following equation can be expressed like (10)

$$v_C(t) = g_3(v_A, i_A, t) \tag{12}$$

The voltage at the right-hand side of the shunt FACTS device (v_D) is equal to v_C. Consider the DB part of the line, the voltage of bus D (v_D) and the voltage and current of bus B (v_B, i_B) are available. Therefore the described procedure in Section 2.1 can be utilised. Thus, using (12), the following discretised equation is derived similar to (11)

$$\begin{cases} G_2(v_A, i_A, v_B, i_B, x, R_\mathrm{f}, k) = 0 \\ x_\mathrm{Comp} < x < x_\mathrm{Line} \end{cases} \tag{13}$$

where x_Line is the distance between two buses B and A.

Equation (13) is derived under the assumption that the fault occurs on the DB section of the line so, $x_\mathrm{Comp} < x < x_\mathrm{Line}$.

The discretised equations (11) and (13) are utilised to derive an optimisation problem in the next step.

Step three: The double criterion function (14) is defined based on the discretised equations (11) and (13), which have been obtained in the first and second steps

$$G = \begin{cases} G_1(v_A, i_A, v_B, i_B, x, R_\mathrm{f}, k), & 0 < x < x_\mathrm{Comp} \\ G_2(v_A, i_A, v_B, i_B, x, R_\mathrm{f}, k), & x_\mathrm{Comp} < x < x_\mathrm{Line} \end{cases} \tag{14}$$

Equation (14) is valid for all points of the line from the beginning to the end, except for the compensator location; but just at the fault point, (14) results in closest value to zero for all samples in the data window. So, the following optimisation problem is expressed based on (14)

$$\begin{cases} \mathrm{Min}\, J(x, R_f) = \underset{x,R_\mathrm{f}}{\mathrm{Min}} \sum_k G^2(v_A, i_A, v_B, i_B, x, R_\mathrm{f}, k) \\ \text{Subject to: } \begin{cases} 0 \le R_\mathrm{f} \\ 0 < x < x_\mathrm{Line} \\ x \ne x_\mathrm{Comp} \end{cases} \end{cases} \tag{15}$$

The fault resistance is a positive number, thus the constraint $R_\mathrm{f} \ge 0$ is added to the optimisation problem. Solving (15), the optimisation problem offers the solution (x_F, R_F), where x_F is the exact location of fault and R_F is the fault resistance. Therefore the fault location and the correct side of it are determined simultaneously and proposing a selector is not needed.

Since x is limited between 0 and x_Line, this optimisation problem can be solved using the enumeration method. Thus, the objective function values are calculated for all x values along the line by a step of Δx, which is an arbitrary number and then the minimum of the objective function values is chosen to solve the problem and find the fault location. For example, choose $\Delta x = 1$ km, then set $x = 1$ km, now (11) has one unknown quantity, that is, R_f. Using the least square estimation method, the fault resistance R_f1 is achieved from (11) for $x = 1$ km, and the objective function value $J(1, R_\mathrm{f1})$ is calculated by using (15). Then, x is increased to 2 km by the step of Δx and (11) is solved again using the least square estimation method, and the objective function value $J(2, R_\mathrm{f2})$ is calculated again by using (15) for $x = 2$ km. This procedure is continued until $x = x_\mathrm{Comp} - \Delta x$ and the objective function values are calculated for all x values within the span of $0 < x < x_\mathrm{Comp}$. The same procedure is performed for the second part of the line ($x_\mathrm{Comp} < x < x_\mathrm{Line}$), but the difference is that (13) is utilised instead of (11). Hitherto, the objective function values are calculated for all x values within the span of $0 < x < x_\mathrm{Line}$. Now the optimisation problem is solved by choosing the minimum of these values. It is worthy to note that, to obtain more accurate optimum value while executing the algorithm, Δx can be chosen smaller than that selected above, for example, 0.1 km.

Considering preceding description, it is quite obvious that solving the fault location problem avoids iterative calculations and, in addition, the algorithm does not need to propose a selector. Also as obtained from (15), solving the optimisation problem only needs the sending and receiving end recorded data and there is no any dependency on the model of the shunt compensator. These are the salient advantages of the proposed algorithm.

2.3 Unsymmetrical three-phase faults

In a three-phase transmission line, the voltages and currents of the line are related to self- and mutual coupling distributed parameters of the phases and this relation is expressed by the partial differential equations in the time domain [15]. A transformation such as Karrenbauer, Wedepohl and Clark can be used to decompose the partial differential equations of a transposed line into their modal components. Hence, the derivation procedure outlined previously for the symmetrical three-phase faults is applicable to each of these modal components and the solutions for other fault types can be simply derived. Subsequently, the proposed method is described for a single- phase-to-ground fault as a typical of unsymmetrical faults.

2.3.1 Single-phase-to-ground fault: In this case, a-phase to ground fault is considered. To develop the fault location algorithm, three steps should be executed. In the first step, assume that the fault occurs on the left-hand side of the compensator (Fig. 1). Since the voltage is continuous along the line, the following set of equations can be expressed at the fault point for phases a, b and c

$$\begin{cases} v^a_{FC}(t) = v^a_{FA}(t) \\ v^b_{FC}(t) = v^b_{FA}(t) \\ v^c_{FC}(t) = v^c_{FA}(t) \end{cases} \tag{16}$$

where $v^a_{FC}(t)$, $v^b_{FC}(t)$ and $v^c_{FC}(t)$ are the voltages at the right-hand side of the fault point for the phases a, b and c, respectively; $v^a_{FA}(t)$, $v^b_{FA}(t)$ and $v^c_{FA}(t)$ are the voltages at the left-hand side of the fault point for the phases a, b and c, respectively.

The following modal equation is resulted for kth mode, by applying the Karrenbauer transformation matrix for (16)

$$v^{(k)}_{FC}(t) = v^{(k)}_{FA}(t) \quad k = 0, 1, 2 \tag{17}$$

In other words, the modal voltages at the left-hand side of the fault point are equal to the modal voltages at the right-hand side of it. Based on the Kirchhoff's current law, the following set of equations is obtained at the fault point, considering a-phase to ground fault

$$\begin{cases} i^a_{FC}(t) = -i^a_{FA}(t) - \dfrac{v^a_{FA}(t)}{R_\mathrm{f}} \\ i^b_{FC}(t) = -i^b_{FA}(t) \\ i^c_{FC}(t) = -i^c_{FA}(t) \end{cases} \tag{18}$$

where $i^a_{FC}(t)$, $i^b_{FC}(t)$ and $i^c_{FC}(t)$ are the currents at the right-hand side of the fault for the phases a, b and c respectively;

doi: 10.1049/iet-gtd.2011.0657

and $i^a_{FA}(t)$, $i^b_{FA}(t)$ and $i^c_{FA}(t)$ are the currents at the left-hand side of the fault for the phases a, b and c, respectively.

Applying the Karrenbauer transformation matrix for (18), the following modal equation is written for the kth mode

$$i^{(k)}_{FC}(t) = -i^{(k)}_{FA}(t) - \frac{v^a_{FA}(t)}{3R_f} \quad k = 0, 1, 2 \qquad (19)$$

Using (19) instead of (3), a discretised equation is obtained in the first step, for the kth mode similar to (11). The procedure for the second step is similar to the step one. Finally, in step three, an optimisation problem like (15) is derived from the first two steps, and then, the exact location of fault is obtained by solving it.

To evaluate the accuracy of the proposed algorithm the following section is illustrated.

3 Performance evaluation

Since the model of shunt compensator is not used in the proposed algorithm, this method is suitable for any transmission line compensated by any shunt device, which does not include a series branch. In principle, a STATCOM performs the same voltage regulation function as the SVC but in a more robust manner and it is better able to provide reactive/current support for a supply system whose voltage is severely depressed [12, 16]. However, a 300 km, 345 kV transmission line compensated by a STATCOM (shown in Fig. 1) is used to evaluate the accuracy of the proposed algorithm by the PSCAD/EMTDC simulator. The parameters of the simulated system are presented in the appendix. For the simulation study, a three-level, 12-pulse STATCOM is considered. The STATCOM is connected into the transmission system through an 11 kV/345 kV, Δ/Y transformer. A slope of 3% is employed in its characteristic and a three-phase balanced firing scheme is adopted. The STATCOM is operated in voltage control mode with a proportional integral (PI) controller to regulate the voltage at its point of connection to the setting value V_{ref}, during steady-state operating conditions.

To evaluate the accuracy of the presented method itself, the instrument transformers have been primarily modelled as ideal devices and the synchronisation error is ignored. The error of the fault location is expressed in terms of percentage of the total line length as follows

$$\%\ \text{error} = \frac{\text{calculated distance} - \text{actual distance}}{\text{line length}} \times 100 \qquad (20)$$

As an example, a three-phase fault occurs at the distance of 144.5 km from the sending end and its resistance is assumed to be 10 Ω, whereas the STATCOM is installed at 140 km from the sending end. In this case, the optimisation problem (15) should be solved. For more accuracy, Δx is chosen 0.1 km and the objective function values are calculated for all x values within the span of $0 < x < 300$ km except for $x = 140$ km by the step of Δx. The result of running the algorithm (by solving the optimisation problem (15)) is

$$(x_F, R_F) = (144.5\,\text{km}, 10.002\ \Omega)$$

So, the fault location error is 0.0%.

The accuracy of the algorithm is also evaluated in the following.

Table 1 Effect of fault types and resistances on the accuracy of the proposed method

Fault type	Actual location of fault, km	$R_f = 1\ \Omega$		$R_f = 10\ \Omega$		$R_f = 100\ \Omega$	
		Calculated location of fault, km	Error, %	Calculated location of fault, km	Error, %	Calculated location of fault, km	Error, %
single phase to ground	20	19.92	−0.0267	20.02	0.0067	20.02	0.0067
	70	69.96	−0.0133	70.07	0.0233	70.07	0.0233
	130	129.96	−0.0133	130	0	130.02	0.0067
	150	150	0	149.98	−0.0067	149.96	−0.0133
	220	220.08	0.0267	219.92	−0.0267	220.03	0.01
	280	280.08	0.0267	279.98	−0.0067	279.98	−0.0067
three phase to ground	20	20.02	0.0067	20.02	0.0067	20.10	0.0333
	70	70	0	70.07	0.0233	70.05	0.0167
	130	130.06	0.02	130	0	130.05	0.0167
	150	149.92	−0.0267	149.98	−0.0067	149.96	−0.0133
	220	220.08	0.0267	219.92	−0.0267	219.90	−0.0333
	280	280.08	0.0267	279.98	−0.0067	279.90	−0.0333
double phase to ground	20	19.92	−0.0267	20.02	0.0067	20.02	0.0067
	70	69.96	−0.0133	70.07	0.0233	70.07	0.0233
	130	129.96	−0.0133	130	0	130.02	0.0067
	150	150	0	149.98	−0.0067	149.96	−0.0133
	220	220.08	0.0267	219.92	−0.0267	220.03	0.01
	280	280.08	0.0267	279.98	−0.0067	279.98	−0.0067
double phase	20	19.92	−0.0267	20.02	0.0067	20.02	0.0067
	70	69.96	−0.0133	70.07	0.0233	70.07	0.0233
	130	129.96	−0.0133	130	0	130.02	0.0067
	150	150	0	149.98	−0.0067	149.96	−0.0133
	220	220.08	0.0267	219.92	−0.0267	220.03	0.01
	280	280.08	0.0267	279.98	−0.0067	279.98	−0.0067

3.1 Sensitivity to the fault resistance and the fault inception angle

Sensitivity analyses of the proposed fault location method to the fault resistance and to the fault inception angle have been performed and the summary results are presented in Tables 1 and 2, respectively. As seen from these tables, the maximum absolute error is 0.0267 and 0.0333%, respectively.

In addition, for accuracy evaluation of the presented method, statistical studies have been performed with over 1920 different random test cases obtained from the PSCAD/EMTDC simulator for different fault types (a–g, a–b, a–b–g and a–b–c–g). Test cases have been considered by random distribution of the following:

- eight fault locations (between 0 and 300 km);
- five fault resistances (between 0 and 100 Ω);
- four inception angles (between 0° and 180°);
- three STATCOM locations (between 0 and 300 km).

Statistical results of the fault location errors show that the absolute error does not exceed 0.0454% and the maximum absolute error happens while a–g fault occurs at 153.364 km from the sending end and the fault resistance is 100 Ω. The average of the absolute errors is about 0.0124% for all cases.

From Tables 1 and 2 and the statistical results, it can be concluded that the proposed algorithm is not sensitive to the fault location, fault type, fault resistance, fault inception angle and the shunt compensator location, and a very good accuracy of the fault location is achieved by using the proposed method. The maximum absolute error in the fault location does not exceed 0.0454% in these cases, and it is definitely acceptable.

3.2 Sensitivity to measurement errors

Hitherto, instrument transformers are modelled errorless; however practically, the conventional instrument transformers may add errors to measurements. For comprehensive evaluation, it is useful to investigate the sensitivity analysis of the proposed algorithm to measurement errors [10]. Thus, the voltage and current samples obtained from PSCAD/EMTDC are subjected to perturbations, and then are fed into the fault location algorithm. The STATCOM is installed at the same location as the case one, and single-phase-to-ground fault is considered and the fault resistance is selected as 10 Ω.

To study the influence of the errors in the voltage and/or current data on the accuracy of the proposed method for different fault locations, the voltage and/or current samples at buses *A* and/or *B* are perturbed by an error of −5% or +5%. The obtained fault location errors are summarised in Table 3. In this study, except for the perturbed measurements, other measurements are assumed to be errorless. In Table 3, at the first four rows, the voltage or current samples at bus *A* are perturbed by an error of −5% or +5%. When the fault happens on the right-hand side of the compensator, the measurement errors have the least influence on the proposed method. The maximum absolute error is 1.23% that is smaller than the measurement error. At the second eight rows of Table 3, the error of the fault location algorithm is shown, when the errors of −5% and/or +5% have been added to the voltage or current samples of buses *A* and *B*. At the last two rows, the voltage samples

Table 2 Effect of fault inception angles on the accuracy of the proposed method

Fault type	Actual location of fault, km	Inception angle = 0°		Inception angle = 45°		Inception angle = 90°	
		Calculated location of fault, km	Error, %	Calculated location of fault, km	Error, %	Calculated location of fault, km	Error, %
single phase to ground	20	20.1	0.0333	20.02	0.0067	20.02	0.0067
	70	70.05	0.0167	69.96	−0.0133	70.07	0.0233
	130	130.05	0.0167	130.02	0.0067	130	0
	150	150	0	149.96	−0.0133	149.98	−0.0067
	220	219.9	−0.0333	220.03	0.01	219.92	−0.0267
	280	279.9	−0.0333	279.98	−0.0067	279.98	−0.0067
three phase to ground	20	20.1	0.0333	20.02	0.0067	20.02	0.0067
	70	70.05	0.0167	70.07	0.0233	70.07	0.0233
	130	130.05	0.0167	130.02	0.0067	130	0
	150	150	0	149.96	−0.0133	149.98	−0.0067
	220	219.9	−0.0333	220.03	0.01	219.92	−0.0267
	280	279.9	−0.0333	279.98	−0.0067	279.98	−0.0067
double phase to ground	20	20.1	0.0333	20.02	0.0067	20.02	0.0067
	70	70.05	0.0167	70.07	0.0233	70.07	0.0233
	130	130.05	0.0167	130.02	0.0067	130	0
	150	150	0	149.96	−0.0133	149.98	−0.0067
	220	219.9	−0.0333	220.03	0.01	219.92	−0.0267
	280	279.9	−0.0333	279.98	−0.0067	279.98	−0.0067
double phase	20	20.1	0.0333	20.02	0.0067	20.02	0.0067
	70	70.05	0.0167	69.96	−0.0133	70.07	0.0233
	130	130.05	0.0167	130.02	0.0067	130	0
	150	150	0	149.96	−0.0133	149.98	−0.0067
	220	219.9	−0.0333	220.03	0.01	219.92	−0.0267
	280	279.9	−0.0333	279.98	−0.0067	279.98	−0.0067

doi: 10.1049/iet-gtd.2011.0657

Table 3 Estimation of sensitivity to measurement errors with different locations of fault

Error in measurements	Actual location of fault, km					
	20	70	130	150	220	280
	Fault location error, %					
−5% error in v_A	−0.33	−1.10	−0.40	0.03	0	0
+5% error in v_A	0.33	1.03	0.06	0	0.03	0
−5% error in i_A	0.37	1.23	0.27	0.03	0.03	0.03
+5% error in i_A	−0.33	−1.13	−0.43	0	−0.03	−0.03
−5% error in v_A and v_B	−0.33	−1.20	−0.60	−0.10	1.27	0.33
−5% error in v_A and +5% in v_B	−0.30	−1.10	−0.30	0.13	−1.17	−0.33
−5% error in i_A and i_B	0.37	1.27	0.30	0.17	−1.27	−0.33
−5% error in i_A and +5% in i_B	0.33	1.20	0.17	−0.03	1.20	0.30
+5% error in v_A and v_B	0.33	1.20	0.27	0.17	−1.20	−0.33
+5% error in v_A and −5% in v_B	0.33	1.07	0.10	−0.07	1.23	0.33
+5% error in i_A and i_B	−0.33	−1.13	−0.53	−0.10	1.20	0.30
+5% error in i_A and −5% in i_B	−0.30	−1.13	−0.33	−0.10	−1.30	−0.33
+5% error in v_A and v_B, −5% error in i_A and i_B	0.70	2.53	0.40	0.73	−2.43	−0.67
−5% error in v_A and v_B, +5% error in i_A and i_B	−0.63	−2.33	−1.77	−0.20	2.43	0.53

of buses A and B are perturbed by the error of −5% and/or +5%, and the current samples are also perturbed similarly. As shown in this part of Table 3, the maximum absolute error is 2.53% and it happens when the voltage samples are perturbed in opposite direction of the current samples, that is, +5% error is added to the voltage samples and −5% error is added to the current samples. It can also be seen from this table that the maximum absolute error does not exceed 2.54% in all cases in which the measurement errors exist.

The same studies have been performed for the other fault types and the results have been obtained similarly. The maximum absolute error has been kept below 3.1% considering ±5% measurement errors in all test cases, which is less than the perturbation in the measurements. To save space, the details are not included.

3.3 Sensitivity to synchronisation error

To consider the effect of synchronisation error on the fault location accuracy, simulation examples with respect to different fault resistances and various random fault locations have been performed for single-phase-to-ground fault. A synchronisation error of −10°, −5°, 5° and 10° has been added to the measurements at terminal A and the results are shown in Table 4. It can be concluded that the accuracy of the algorithm is high for low fault resistances. When the fault resistance is 50 Ω, and the synchronisation error is 10°, it will cause up to 0.1487% absolute error in the fault location, whereas the fault occurs at 59.046 km from the sending end. For larger fault resistances, it has been found that the effect of synchronisation error is severe on the fault location accuracy.

3.4 Sensitivity to line parameters error

In this test, the effect of error in the line parameters on the fault location accuracy is evaluated. The, inductance (L), capacitance (C) and resistance (R) of the line are subjected to ±10% variation about the true values. Then, the perturbed line parameters are fed into the proposed fault location algorithm and the results are presented in Table 5, whereas the fault resistance is assumed to be 10 Ω. This table shows that the line parameter errors influence the fault location accuracy, such that a −10% error in the line capacitance (C) can only cause a maximum absolute error of 1.46% in the fault location while the fault occurs at 222.379 km from the sending end.

3.5 Sensitivity to untransposed line

In this case, the line is considered untransposed and is subjected to different fault conditions. For untransposed lines, it is notable that the transformation matrix can also be found to transform the coupled phase quantities to decoupled modal quantities with eigenvalue/eigenvector

Table 4 Effect of synchronisation errors on the accuracy of the proposed method

Actual location of fault, km	Fault resistance, Ω	Fault location error, %			
		Synch. error = −10°	Synch. error = −5°	Synch. error = 5°	Synch. error = 10°
59.046	1	−0.0153	−0.0153	−0.0153	−0.0153
	10	−0.0153	−0.0153	−0.0153	−0.0153
	30	0.018	−0.0487	0.0180	−0.0487
	50	0.0513	−0.1487	−0.0153	−0.1487
222.379	1	0.007	0.007	0.007	0.007
	10	−0.0263	0.007	0.007	0.007
	30	−0.0597	−0.0263	−0.0263	−0.0263
	50	−0.093	−0.0263	−0.0263	−0.0930

Table 5 Effect of line parameters error on the accuracy of the proposed algorithm

Fault type	Actual location of fault, km	Fault location error, %				
		+10% error in L	−10% error in L	+10% error in C	−10% error in C	±10% error in R
single phase to ground	59.046	−0.882	1.018	−0.950	1.085	−0.015
	222.379	1.174	−1.360	1.240	−1.426	0.007
three phase to ground	59.046	−0.915	1.018	−0.950	1.085	−0.015
	222.379	1.174	−1.326	1.240	−1.460	0.007
double phase to ground	59.046	−0.915	1.051	−0.950	1.085	−0.015
	222.379	1.174	−1.326	1.240	−1.460	0.007
double phase	59.046	−0.915	1.018	−0.915	1.118	−0.015
	222.379	1.174	−1.326	1.240	−1.460	0.007

Table 6 Effect of fault types and resistances on the accuracy of the proposed method considering untransposed transmission line

Fault type	Actual location of fault, km	Fault location error, %		
		$R_f = 1\ \Omega$	$R_f = 10\ \Omega$	$R_f = 100\ \Omega$
single phase to ground	59.046	−0.0153	−0.0153	−0.0153
	222.379	0.007	0.007	0.007
three phase to ground	59.046	−0.0153	−0.0153	−0.0153
	222.379	0.007	0.007	0.007
double phase to ground	59.046	−0.0153	−0.0153	−0.0153
	222.379	0.007	0.007	0.007
double phase	59.046	−0.0153	−0.0153	−0.0153
	222.379	0.007	0.007	0.007

theory [15]. Thus, an optimisation problem like (15) is derived which is utilised for the fault location. The results of running the proposed method are reported in Table 6 for an untransposed transmission line compensated by the STATCOM. Based on the presented results in this table, it can be seen that the novel method is also accurate when an untransposed transmission line is taken into consideration.

4 Conclusion

In this paper, a novel non-iterative fault location algorithm for the transmission lines compensated by the shunt FACTS devices is proposed. In the presented method, synchronised data of two ends of the transmission line are used and distributed parameter line model in time domain is applied. Two discretised equations are used to derive the optimisation problem and the side and the location of fault and its resistance are determined simultaneously by solving this problem. Thus, the algorithm does not need to propose a selector to determine the section of fault and it does not require iterative calculations. Since the proposed method does not use the model of the shunt compensator for the fault location, it is suitable for any transmission line included each type of shunt device, and the compensator model parameters do not influence the fault location technique. The STATCOM is considered for simulation in PSCAD/EMTDC to evaluate the accuracy of the proposed method. The simulation results verify the high accuracy of the algorithm and the maximum absolute error of fault location does not exceed 0.0454% without considering errors in the measurements, synchronisation and line parameters. This is so, since the new method offers a very accurate analytical time domain based fault location algorithm, in which the distributed parameter line model is applied. The method is also evaluated considering errors in the measurements, synchronisation and line parameters.

5 References

1 Suonan, J., Qi, J.: 'An accurate fault location algorithm for transmission line based on R–L model parameter identification', *Electr. Power Syst. Res.*, 2005, **76**, pp. 17–24

2 Sadeh, J., Ranjbar, A.M., Hadjsaid, N., Feuillet, R.: 'Accurate fault location algorithm for power transmission lines', *Eur. Trans. Electr. Power*, 2000, **10**, (5), pp. 313–318

3 Mardiana, R., Motairy, H.A., Su, C.Q.: 'Ground fault location on a transmission line using high-frequency transient voltages', *IEEE Trans. Power Deliv.*, 2011, **26**, (2), pp. 1298–1299

4 Kezunovic, M., Mrkic, J., Perunicic, B.: 'An accurate fault location algorithm using synchronized sampling', *Electr. Power Syst. Res.*, 1994, **29**, pp. 161–169

5 Jiang, J.A., Yang, J.Z., Lin, Y.H., Liu, C.W., Ma, J.C.: 'An adaptive PMU based fault detection/location technique for transmission lines – part I: theory and algorithms', *IEEE Trans. Power Deliv.*, 2000, **15**, (2), pp. 486–493

6 Xu, Z.Y., Jiao, S.H., Ran, L., Du, Z.Q.: 'An online fault-locating scheme for EHV/UHV transmission lines', *IET Gener. Transm. Distrib.*, 2008, **2**, (6), pp. 789–799

7 Radojević, Z.M., Kim, C.H., Popov, M., Preston, G., Terzija, V.: 'New approach for fault location on transmission lines not requiring line parameters'. Int. Conf. on Power Systems Transients (IPST2009), Kyoto, Japan, June 2009

8 Preston, G., Radojević, Z.M., Kim, C.H., Terzija, V.: 'New settings-free fault location algorithm based on synchronised sampling', *IET Gener. Transm. Distrib.*, 2011, **5**, (3), pp. 376–383

9 Novosel, D., Hart, D.G., Udren, E., Garitty, J.: 'Unsynchronized two-terminal fault location estimation', *IEEE Trans. Power Deliv.*, 1996, **11**, (1), pp. 130–138

10 Liao, Y.: 'Unsynchronized fault location based on distributed parameter line model', *Electr. Power Compon. Systems*, 2007, **35**, (9), pp. 1061–1077

11 Izykowski, J., Rosolowski, E., Balcerek, P., Fulczyk, M., Saha, M.M.: 'Accurate noniterative fault location algorithm utilizing two-end unsynchronized measurements', *IEEE Trans. Power Deliv.*, 2010, **25**, (1), pp. 72–80

doi: 10.1049/iet-gtd.2011.0657

12 Song, Y.H., Johns, A.T.: 'Flexible AC transmission systems (FACTS)' (The Institution of Electrical Engineers, London, UK, 1999)
13 Naghdi, M., Sadeh, J., Ghazi, R.: 'Fault location in transmission lines compensated by shunt facts devices' (in Persian)'. 16th Iranian Conf. Electrical Engineering (ICEE2008), Tehran, Iran, 2008
14 Sadeh, J., Hadjsaid, N., Ranjbar, A.M., Feuillet, R.: 'Accurate fault location for series compensated transmission lines', *IEEE Trans. Power Deliv.*, 2000, **15**, (3), pp. 1027–1033
15 Johns, A.T., Salman, S.K.: 'Digital protection for power systems' (Peter Peregrinus Ltd, London, UK, 1995)
16 Acha, E., Fuerte-Esquivel, C.R., Ambriz-Perez, H., Angeles-Camacho, C.: 'FACTS, modelling and simulation in power network' (John Wiley & Sons Ltd, The Atrium, Southern Gate, Chichester, UK, 2004)

6 Appendix: system data

Power system:

System nominal voltage = 345 (kV);
System nominal frequency = 60 (Hz);
Phase angle between voltage sources = 25°.

Transmission line:

1. Zero-sequence: $R_0 = 0.275$ (Ω/km), $L_0 = 3.4505998$ (mH/km) and $C_0 = 8.5$ (nF/km).
2. Positive-sequence: $R_1 = 0.0275$ (Ω/km), $L_1 = 1.002768$ (mH/km) and $C_1 = 13$ (nF/km).

STATCOM:

1. Capacitance: two 300 μF; and
2. Transformer: rating = 200 (MVA), ratio = 11 (kV)/345 (kV).